



**Universiteit
Leiden**
The Netherlands

Partial loss of USP9X function leads to a male neurodevelopmental and behavioral disorder converging on transforming growth factor beta signaling

Johnson, B.V.; Kumar, R.; Oishi, S.; Alexander, S.; Kasherman, M.; Vega, M.S.; ... ; S

Citation

Johnson, B. V., Kumar, R., Oishi, S., Alexander, S., Kasherman, M., Vega, M. S., ... Shields, K. (2020). Partial loss of USP9X function leads to a male neurodevelopmental and behavioral disorder converging on transforming growth factor beta signaling. *Biological Psychiatry*, 87(2), 100-112. doi:10.1016/j.biopsych.2019.05.028

Version: Publisher's Version
License: [Creative Commons CC BY 4.0 license](https://creativecommons.org/licenses/by/4.0/)
Downloaded from: <https://hdl.handle.net/1887/3181481>

Note: To cite this publication please use the final published version (if applicable).

Partial Loss of USP9X Function Leads to a Male Neurodevelopmental and Behavioral Disorder Converging on Transforming Growth Factor β Signaling

Brett V. Johnson, Raman Kumar, Sabrina Oishi, Suzy Alexander, Maria Kasherman, Michelle Sanchez Vega, Atma Ivancevic, Alison Gardner, Deepti Domingo, Mark Corbett, Euan Parnell, Sehyoun Yoon, Tracey Oh, Matthew Lines, Henrietta Lefroy, Usha Kini, Margot Van Allen, Sabine Grønberg, Sandra Mercier, Sébastien Küry, Stéphane Bézieau, Laurent Pasquier, Martine Raynaud, Alexandra Afenjar, Thierry Billette de Villemeur, Boris Keren, Julie Désir, Lionel Van Maldergem, Martina Marangoni, Nicola Dikow, David A. Koolen, Peter M. VanHasselt, Marjan Weiss, Petra Zwijnenburg, Joaquim Sa, Claudia Falcao Reis, Carlos López-Otín, Olaya Santiago-Fernández, Alberto Fernández-Jaén, Anita Rauch, Katharina Steindl, Pascal Joset, Amy Goldstein, Suneeta Madan-Khetarpal, Elena Infante, Elaine Zackai, Carey Mcdougall, Vinodh Narayanan, Keri Ramsey, Saadet Mercimek-Andrews, Loren Pena, Vandana Shashi, Undiagnosed Diseases Network, Kelly Schoch, Jennifer A. Sullivan, Filippo Pinto e Vairo, Pavel N. Pichurin, Sarah A. Ewing, Sarah S. Barnett, Eric W. Klee, M. Scott Perry, Mary Kay Koenig, Catherine E. Keegan, Jane L. Schuette, Stephanie Asher, Yezmin Perilla-Young, Laurie D. Smith, Jill A. Rosenfeld, Elizabeth Bhoj, Paige Kaplan, Dong Li, Renske Oegema, Ellen van Binsbergen, Bert van der Zwaag, Marie Falkenberg Smeland, Ioana Cutcutache, Matthew Page, Martin Armstrong, Angela E. Lin, Marcie A. Steeves, Nicolette den Hollander, Mariëtte J.V. Hoffer, Margot R.F. Reijnders, Serwet Demirdas, Daniel C. Koboldt, Dennis Bartholomew, Theresa Mihalic Mosher, Scott E. Hickey, Christine Shieh, Pedro A. Sanchez-Lara, John M. Graham Jr., Kamer Tezcan, G.B. Schaefer, Noelle R. Danylchuk, Alexander Asamoah, Kelly E. Jackson, Naomi Yachelevich, Margaret Au, Luis A. Pérez-Jurado, Tjitske Kleefstra, Peter Penzes, Stephen A. Wood, Thomas Burne, Tyler Mark Pierson, Michael Piper, Jozef Gécz, and Lachlan A. Jolly

ABSTRACT

BACKGROUND: The X-chromosome gene *USP9X* encodes a deubiquitylating enzyme that has been associated with neurodevelopmental disorders primarily in female subjects. *USP9X* escapes X inactivation, and in female subjects de novo heterozygous copy number loss or truncating mutations cause haploinsufficiency culminating in a recognizable syndrome with intellectual disability and signature brain and congenital abnormalities. In contrast, the involvement of *USP9X* in male neurodevelopmental disorders remains tentative.

METHODS: We used clinically recommended guidelines to collect and interrogate the pathogenicity of 44 *USP9X* variants associated with neurodevelopmental disorders in males. Functional studies in patient-derived cell lines and mice were used to determine mechanisms of pathology.

RESULTS: Twelve missense variants showed strong evidence of pathogenicity. We define a characteristic phenotype of the central nervous system (white matter disturbances, thin corpus callosum, and widened ventricles); global delay with significant alteration of speech, language, and behavior; hypotonia; joint hypermobility; visual system defects; and other common congenital and dysmorphic features. Comparison of in silico and phenotypical features align additional variants of unknown significance with likely pathogenicity. In support of partial loss-of-function mechanisms, using patient-derived cell lines, we show loss of only specific *USP9X* substrates that regulate neurodevelopmental signaling pathways and a united defect in transforming growth factor β signaling. In addition, we find correlates of the male phenotype in *Usp9x* brain-specific knockout mice, and further resolve loss of hippocampal-dependent learning and memory.

CONCLUSIONS: Our data demonstrate the involvement of *USP9X* variants in a distinctive neurodevelopmental and behavioral syndrome in male subjects and identify plausible mechanisms of pathogenesis centered on disrupted transforming growth factor β signaling and hippocampal function.

Keywords: Brain malformation, Deubiquitylating enzyme, Hippocampus, Neurodevelopmental disorder, TGF β , USP9X

<https://doi.org/10.1016/j.biopsych.2019.05.028>

USP9X is a highly conserved X-chromosome gene that encodes a substrate-specific deubiquitylating enzyme (1). Complete *Usp9x* loss of function (LOF) is embryonic lethal in mice (2), and homo- or hemizygous complete LOF germline mutations have never been identified in humans. We previously reported the identification of 17 female individuals with neurodevelopmental disorders (NDDs) due to *USP9X* de novo heterozygous complete LOF mutations (predominately early frame shift and/or stop gain mutations) (3). *USP9X* escapes X inactivation, and in these individuals the messenger RNA and protein levels are significantly reduced. The phenotype is recognizable, and it involves intellectual disability (ID), structural brain abnormalities, characteristic facial features, and distinctive congenital malformations (3). We also reported 2 missense variants and a truncating frame shift variant (escaping nonsense-mediated messenger RNA decay) associated with male ID (4). These variant proteins retained core enzymatic activity and instead impaired specific USP9X brain functions, including neuronal migration and growth (4). Two additional novel missense variants were also implicated in epilepsy, one de novo and likely pathogenic and another of unknown significance (5). Thus, the involvement of *USP9X* remains only tentatively associated with nonspecific male NDDs.

USP9X has a central deubiquitylating catalytic domain and long N- and C-terminal extensions used to mediate substrate recognition (1). *USP9X* interacts with at least 53 proteins, each in a tissue- and context-dependent manner. *USP9X* deubiquitylates substrates, typically antagonizing their proteasomal degradation and as such stabilizing their levels (1). In the brain, many *USP9X* substrates are encoded by NDD-associated genes (1), while others regulate neurodevelopmental signaling pathways including transforming growth factor β (TGF β), Notch, Wnt, and mammalian target of rapamycin (mTOR) pathways (6–15). Conditional deletion of *Usp9x* in the embryonic forebrain alters these signaling pathways and causes defective neural progenitor cell function, neuronal cell growth, and cell maturation (4,7,12,16–18). Prominent anatomical features of these mice include agenesis of the corpus callosum and loss of postnatal hippocampal growth (17,18). Establishing behavioral phenotypes of these mice is critical to establishing models of human NDDs involving *USP9X*.

Here we interrogate 44 additional *USP9X* missense variants in male participants with NDDs, establish a characteristic clinical phenotype, and resolve key features in knockout mice. We use patient-derived cell lines to discover molecular mechanisms involving neurodevelopmental signaling pathways. Our data underscore the relevance of partial LOF effect

of human *USP9X* variants and point to a loss of TGF β signaling and hippocampal function as major contributors to pathology.

METHODS AND MATERIALS

Participants

This study was approved by the Women's and Children's Health Network Human Research Ethics Committee, South Australia, Australia (HREC786–07–2020). All participant information was provided following informed parental consent (Table S7 in Supplement 1).

Cell Culture

Primary fibroblasts were maintained as previously described (3). TGF β luciferase assays were conducted as previously described (18) in biological quadruplicate using 20 ng/mL TGF β (R&D Systems, In Vitro Technologies, Melbourne, Victoria, Australia). Scratch migration assays were conducted as previously described (19). Number of cells migrating into the scratch was quantified using ImageJ (National Institutes of Health, Bethesda, MD). Assays were blinded to genotype, and biological triplicates were assayed in technical triplicate. TGF β –SMAD family member 4 (SMAD4) localization assay was performed by incubating cells without serum for 8 hours prior to addition of 20 ng/mL TGF β . Assay was conducted blinded to genotype and conducted across 5 experiments.

Immunofluorescence

Immunofluorescence was performed as previously described (20). A list of antibodies is provided in Table S6 in Supplement 1.

Biochemical Analysis

Protein isolation and Western blots were performed as previously described (3). A list of antibodies is provided in Table S6 in Supplement 1. RNA isolation and quantitative polymerase chain reaction was described previously (3).

Proteomics

Immunoprecipitation was as previously described (4). Rabbit immunoglobulin G or anti-USP9X antibody (5 μ g/treatment) (A301-350A; Bethyl Laboratories, Montgomery, TX) were used. Proteins were identified and quantified using tandem-mass-tag 1-dimensional liquid chromatography electrospray ionization tandem-mass-spectrometry by Australian Proteome Analysis Facility (Sydney, Australia). Raw data were searched using Proteome Discoverer version 2.1 (ThermoFisher Scientific,

Waltham, MA) to identify proteins. Raw quantitative values were mean normalized to handle batch effects and logarithmically transformed. Paired *t* tests identified proteins significantly enriched (adjusted *p* < .05 and fold change > 0.5) in USP9X (wild-type and mutant) immunoprecipitates compared with those of immunoglobulin G control subjects.

Mouse Husbandry

Usp9x^{LoxP/LoxP} female mice (129SvJ/C57BL/6 mixed background) and *Emx1-Cre* male mice (C57BL/6 background) were crossed as previously described (17,18). As *Usp9x* is located on the X chromosome, male offspring that inherit the *Emx1-Cre* allele lacked *Usp9x* in the telencephalon and derived cortex and hippocampal structures (referred to as *Usp9x*^{-Y}; *Emx1-Cre* or simply knockout mice). *Cre*-negative male mice were used as controls (referred to as *Usp9x*^{LoxP/Y} or simply wild-type). Female mice were not analyzed.

Open Field Test

Locomotor behavior was assessed in adult mice as previously described (21). Ethovision XT software (Noldus Information Technology, Leesburg, VA) recorded distance traveled over a 30-minute test period and data were assessed in 6 time bins of 5 minutes each.

Primary SHIRPA Screen

Adult mice were screened for gross neurological deficits using a primary SHIRPA (SmithKline Beecham Pharmaceuticals; Harwell, MRC Mouse Genome Centre and Mammalian Genetics Unit; Imperial College School of Medicine at St. Mary's; Royal London Hospital, St. Bartholomew's and the Royal London School of Medicine phenotype assessment) screen (22). Mice were observed in a cylindrical viewing jar for 5 minutes and then transferred to an arena (45 cm × 45 cm), where they underwent a series of anatomical and neurological measures, including assessments of muscular, spinocerebellar, sensory, neuropsychiatric, and autonomic functions.

Active Place Avoidance Task

Adult animals included (6–7 months) *Usp9x*^{-Y}; *Emx1-Cre* (*n* = 17) knockout and *Usp9x*^{LoxP/Y} control subject (*n* = 16) mice. Littermates were raised together regardless of genotype. Test mice were placed onto a rotating platform arena within a room marked by visual cues (23). On entering the stationary shock zone, mice received electric shocks (0.5 mA at 15-ms intervals) until they exited. Habituation consisted of exploration without shock. In each of the following 5 consecutive days, mice were placed on the rotating platform for 10 minutes with active shocks. Data were acquired using Ethovision XT software (Noldus Information Technology). Testing and analysis were performed blinded to genotype. Two-way analysis of variance was performed involving 2 independent variables,

with repeated measures if applicable. Multiple comparisons were adjusted (Bonferroni correction). Statistical significance was set at *p* < .05.

Histology

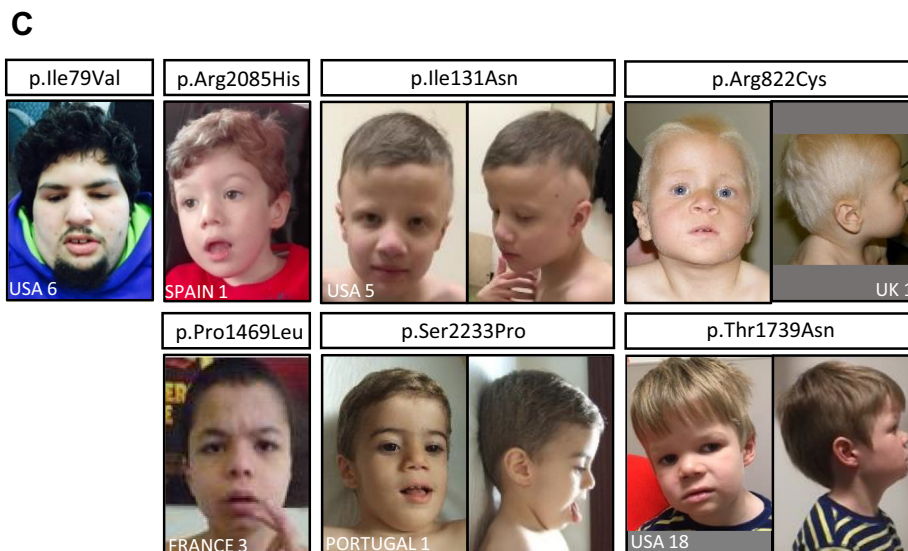
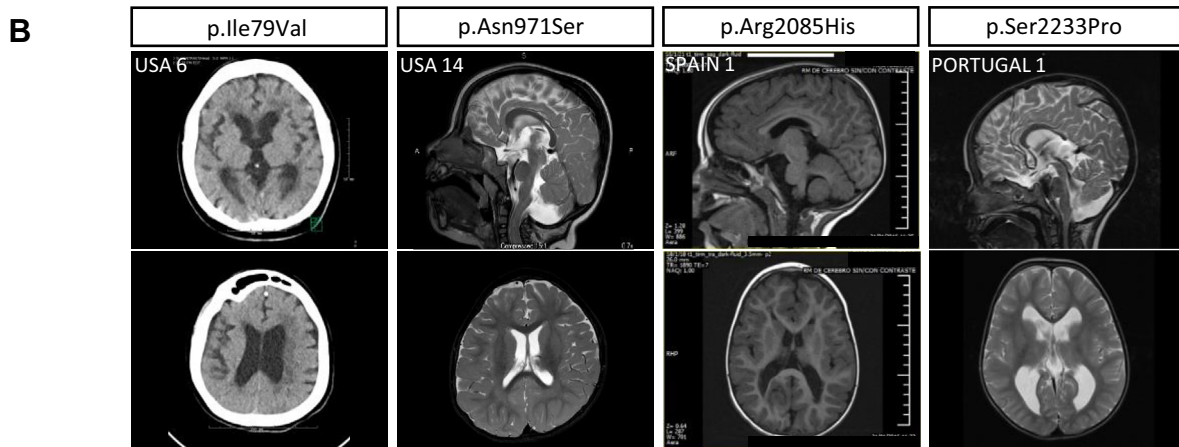
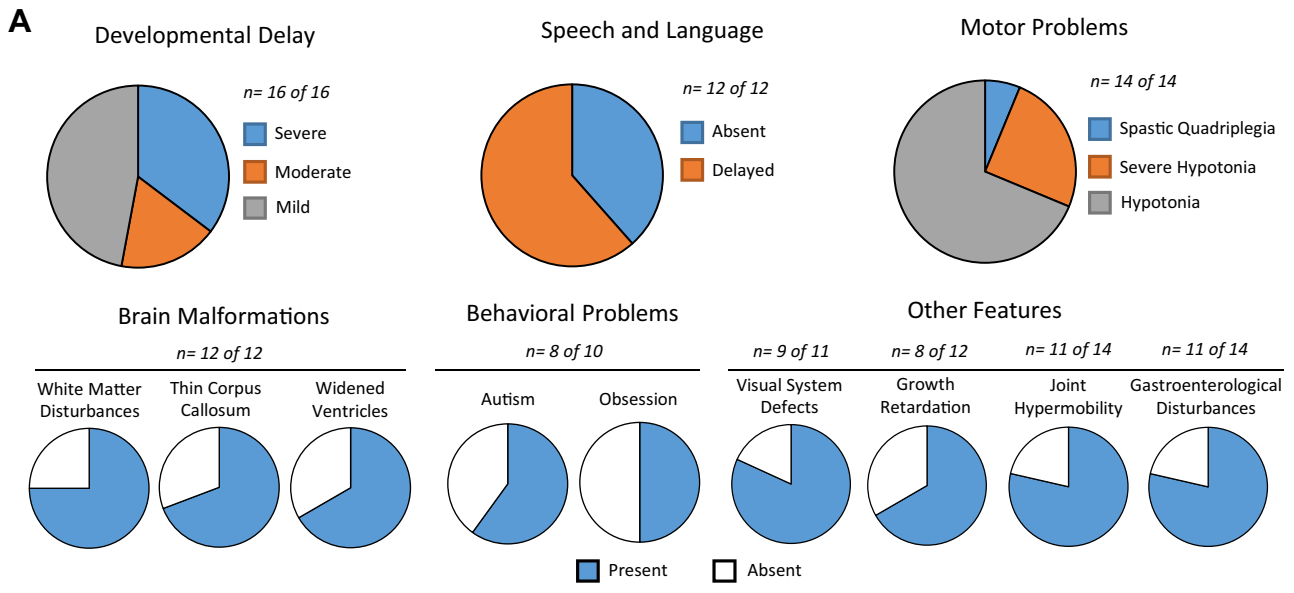
Histology and immunofluorescence testing were conducted as previously described (17).

RESULTS

Identification of De Novo and Inherited USP9X Missense Variants in Affected Male Subjects

Targeting male subjects with NDDs, we discovered 48 cases with 44 unique USP9X variants (3 were recurrent), primarily through trio-based exome sequencing (Table S1 in Supplement 1). Of these, 2 participants were obtained via DECIPHER (<http://decipher.sanger.ac.uk>) (UK1 = DECIPHER patient 260068 and Netherlands 2 = DECIPHER patient 323395) (24). The clinical history of each case is provided in the Supplement. We classified each variant's pathogenicity in accordance with the American College of Medical Genetics and Genomics guidelines (Figure S1 in Supplement 1) (25). Eleven variants (from 13 families) were classified as likely benign (Table S1 in Supplement 1). The remaining 33 variants (from 35 families) were considered the most plausible genetic cause, either because the variant was the sole genetic finding or because it was prioritized over other variants of unknown or unlikely significance (Table S2 in Supplement 1). Nine de novo variants were classified as likely pathogenic (Table S1 and Figures S1 and S2 in Supplement 1). Three of these are located in the catalytic domain; however, structural homology modeling mapped these variants to positions outside of the core catalytic site (Figures S3 and S4 in Supplement 1) (26). The remaining 24 variants (from 26 families) were maternally inherited; segregation beyond trio analysis was able to be performed in 12 of these families (Table S1 in Supplement 1). We conducted functional studies to provide evidence of pathogenicity of 3 such inherited variants (Figure S2 in Supplement 1). Another variant, p.Ala2481fs*17, was recurrent in 3 unrelated cases (Table S1 in Supplement 1). However, this variant affected only the longer of 2 alternative coding USP9X isoforms and was intronic in the short (Figure S5 in Supplement 1). Interpretation was further complicated by the presence of 4 hemizygous alleles in the genome aggregation database gnomAD (Table S1 in Supplement 1). Preferential isoform usage could underlie a variable penetrance, and rare single nucleotide polymorphisms (dbSNP and gnomAD) affecting the 5' donor splice sites exist, but we were unable to classify their involvement beyond variants of unknown significance (VUSs) (Figure S5 in Supplement 1). Thus, from our collection of 44 variants, 12 were likely pathogenic (9 de novo, 3 maternally inherited), 11 likely benign, and 21 VUS (Table S1 and Figure S1 in Supplement 1). The likely

Figure 1. Likely pathogenic USP9X variants cause a characteristic neurodevelopmental disorder in male subjects. **(A)** Constellation and penetrance of defining clinical features. **(B)** Magnetic resonance imaging of the brains of individuals with likely pathogenic USP9X variants. Examples highlight evidence of white matter loss and ventricular widening in all, and in particular periventricular leukomalacia (p.Ile79Val), loss of myelination and/or gliosis of posterior periventricular white matter (p.Asn971Ser), cerebellar vermis hypoplasia (p.Arg2085His), and hypoplastic corpus callosum (p.Ser2233Pro). **(C, D)** Photographs of individuals with USP9X variants. Note short, tapered fingers. *n* = the number of participants whose information contributed to the data.



pathogenic variants altered highly conserved residues and were distributed throughout the protein (Figure S2 in Supplement 1).

USP9X Variants Are Associated With a Spectrum of Neurodevelopmental Features in Male Subjects

We collated clinical information on participants with the 12 likely pathogenic variants and from the 4 previously published male likely pathogenic variants (Table S3 in Supplement 2) (4,5). Global developmental delay or ID, varying from mild to severe, was reported in all cases (Figure 1A). Speech and language problems and motor disability were also found in all cases (where reported). Participants also presented with behavioral issues, predominantly autistic and obsessive behaviors but also attention-deficit/hyperactivity disorder, anxiety, and aggression (Figure 1A). Ophthalmic abnormalities, in particular strabismus, were also prevalent. In all cases where neuroimaging was performed, brain malformations were present that included (but were not limited to) white matter disturbances, hypoplastic corpus callosum, widened ventricles, and cerebellar defects (Figure 1A, B). Outside of the brain, the affected individuals' most common features included joint hypermobility, a range of gastroenterological problems (feeding difficulties, reflux, and constipation, in particular) and growth defects of pre- and postnatal onset (Figure 1A). All affected male participants presented with dysmorphic facial features, although the nature of these varied across the cohort (Figure 1C). Digital defects, mainly tapered and pointed fingers, were also frequently reported (Figure 1D). Collectively, we associate several anomalies of the central nervous system; global delay with significant alteration of speech, language, and behavior; hypotonia; joint hypermobility; strabismus; and some common dysmorphic features with missense *USP9X* variants in male individuals. The prominent neurological features reported in female subjects with *USP9X* variants (3) are frequent in this male cohort; however, other major congenital features of female subjects are infrequent or absent in male subjects (Figure S6 in Supplement 1).

USP9X VUSs Exhibit Features of Pathogenicity

We leveraged our resources of likely pathogenic and benign variants (Table S1 in Supplement 1) and common *USP9X* variants (gnomAD hemizygous variants with allele frequency >1:100,000) to comparatively assess VUSs. There was no clear difference in spatial distribution of variant types across the protein (Figure 2A). Three VUSs located in the catalytic domain were also shown to lie outside of the catalytic site (Figure S4 in Supplement 1). All variants were then compared using ANNOVAR predictive tools (27) to discover algorithms with discriminatory power for *USP9X*. Eight predictive tools were validated, for which 1) common and benign variant scores were similar and 2) common and pathogenic variant scores were significantly different (Figure 2B). These validated tools aligned VUSs more closely with likely pathogenic variants (Figure 2B). CADD and MUT_PRED2 tools employ independent algorithms (28,29), and respective variant scores were moderately correlated (Figure 2C). Combining these scores to predict pathogenicity (CADD >25 and MUT_PRED2 >0.7) enriched for likely pathogenic variants (80% of all likely pathogenic variants) and were accompanied by approximately half

of VUSs (Figure 2C). Similar results were obtained by combining CADD and PROVEAN scores (Figure S7 in Supplement 1).

We also compared the prevalence of the characteristic clinical features in participants with VUSs. Developmental delay, speech and language problems, and behavioral problems were frequent, while other features, including motor problems, brain malformation, and gastroenterological problems (among others), were observed at reduced frequency (Figure S7 in Supplement 1 and Table S4 in Supplement 2). In aggregate, these data reveal in silico and clinical overlap between *USP9X* VUSs with likely pathogenic variants.

USP9X Missense Variants Affect Levels of USP9X and Its Substrates

For 4 maternally inherited variants, we generated patient-derived skin fibroblast cell lines and performed functional studies: USA 6 (p.Ile79Val); France 2 (p.Ala696Val); Portugal 1 (p.Ser2233Pro); and the recurrent frame shift variant from Netherlands 3 (p.Ala2481fs*17). Studies on the p.Ala2481fs*17 variant were uninformative, as the long isoform was barely expressed (Figure S5 in Supplement 1). We investigated the steady-state levels of *USP9X* messenger RNA and protein (Figure 3). The p.Ser2233Pro variant line showed a significant (~50%) reduction of *USP9X* protein level (Figure 3A, B and Figure S8 in Supplement 1). Subcellular localization of *USP9X* variants was not overtly affected (Figure 3C and Figure S9 in Supplement 1).

As complete *Usp9x* LOF is embryonic lethal, we hypothesized that a molecular mechanism of *USP9X* missense variants disrupted only specific subsets of *USP9X* protein-protein interactions rather than all. To test this hypothesis, we immunoprecipitated *USP9X* and interacting proteins from control and variant fibroblast cell lines and subjected them to tandem-mass-tag-based quantitative proteomic analysis (Figure 3D, E and Figure S10 in Supplement 1). We identified 6 proteins (high mobility group nucleosomal binding domain 2 [HMG2], dihydroliipoamide S-acetyltransferase [DLAT], rho-associated protein kinase 2 [ROCK2], potassium channel tetramerization domain containing 9 [KCTD9], formin-binding protein 1-like [FNBP1L], and ribosomal protein S7 [RPS7]) in addition to *USP9X* that were statistically enriched in control *USP9X* IP-over immunoglobulin G (Figure S10 in Supplement 1). Of these interactors, only KCTD9 was significantly depleted (by 20%) in the p.Ile79Val IPs and RPS7 was significantly depleted (by ~40%) in the p.Ala697Val IPs (Figure 3E). We conclude that the variants did not overtly affect most *USP9X* interactions detectable by IP-coupled proteomics.

As *USP9X* is a deubiquitylating enzyme, *USP9X*-substrate interactions are rapid and transient, which can render vigorous detection of interactions refractory to IP. We therefore took a targeted Western blot approach to study the protein expression levels of *USP9X* substrates. We studied substrates specifically involved in neurodevelopmental signaling pathways (Figure 3F, G, and Figure S8 in Supplement 1) (1,4,7,12). All *USP9X* missense variant cell lines had reduced levels of substrates SMAD specific E3 ubiquitin protein ligase 1 (SMURF1), a regulator of TGF β signaling (30), and the activated (hypophosphorylated) form of catenin β -1 (known as CTNNB1

USP9X in Neurodevelopmental and Behavioral Disorders

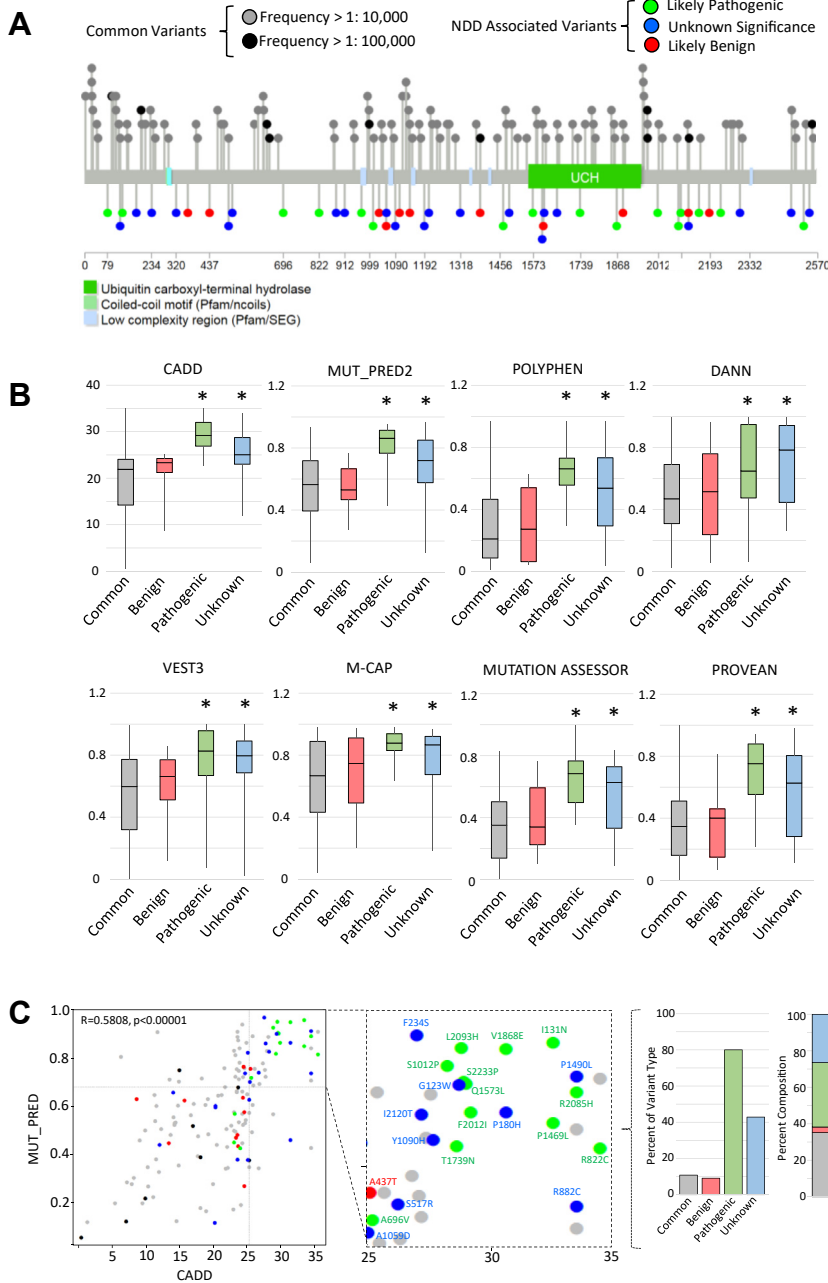


Figure 2. USP9X variants of uncertain significance share in silico signatures with likely pathogenic variants. **(A)** Protein location of ubiquitin specific peptidase 9 X-linked (USP9X) variants and common variants extracted from the gnomAD database. **(B)** Bulk comparison of common, benign, and likely pathogenic variants and variants of unknown significance by a suite of in silico prediction tools. **(C)** Comparison of CADD and MUT_PRED2 scores reveal clustering of variants of unknown significance with likely pathogenic variants in the upper-right quadrant, which is consistent with pathogenicity (CADD > 25, MUT_PRED2 > 0.7). Scores are significantly correlated (Pearson’s correlation given). Color scheme as in panels **(A)** and **(B)**. Inset identifies each variant in the “pathogenic quadrant.” Graphs show percent of each type of variant and the overall composition of variant types within the pathogenic quadrant. *Significantly different from common variants; $p < .05$ by Student’s t test. NDD, neurodevelopmental disorder; Pfam/ncoils, Protein Family Database term coiled-coil regions; Pfam/SEG, Pfam term low complexity region.

or β -Catenin, a regulator of Wnt signaling (31). In addition, total β -Catenin level was significantly reduced in the p.Ile79Val and p.Ser2233Pro cell lines (Figure 3F, G and Figure S8 in Supplement 1). We also found significant reduction of regulatory-associated protein of mTOR (RAPTOR) (mTOR pathway) and myeloid cell leukemia sequence 1 (apoptotic pathway) levels in the p.Ala696Val cell lines ($n = 2$ brothers) (32,33). Other substrates, including itchy E3 ubiquitin protein ligase, mindbomb E3 ubiquitin protein ligase 1, and SMAD4 (regulators of epidermal growth factor, NOTCH, and TGF β

pathways, respectively), were unchanged (Figure 3F and Figure S8 in Supplement 1). Ubiquitylation can also direct the nuclear localization of SMAD4 and β -Catenin, but we failed to identify any major difference in localization under standard culture conditions (Figures S11 and S12 in Supplement 1). Taken together, USP9X missense variants lead to reduced levels of substrates specifically involved in neurodevelopmental signaling pathways, while other more stable and/or robust interactions that were identified via immunoprecipitation were largely unaffected.

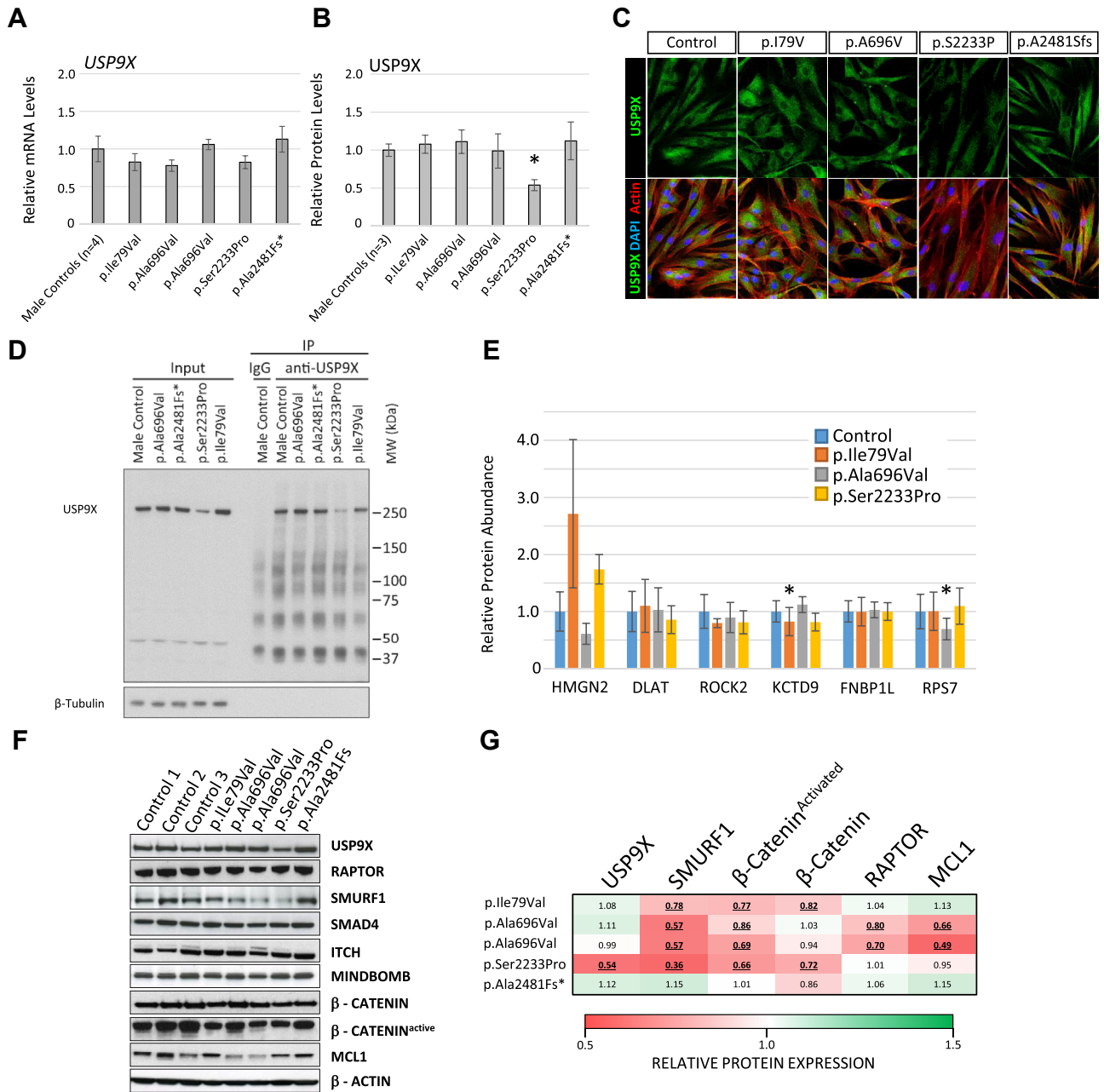


Figure 3. Ubiquitin specific peptidase 9 X-linked (USP9X) variants affect substrates that regulate neurodevelopmental signaling pathways. **(A)** Quantitative real-time polymerase chain reaction of *USP9X* messenger RNA (mRNA) expression in male control and patient-derived fibroblasts. **(B)** Quantitation of $n = 3$ Western blot experiments analyzing protein expression (see Figure S8 in Supplement 1). The p values were calculated via Student's t test. **(C)** Representative immunofluorescence images from control and *USP9X* variant fibroblast cell lines. **(D)** Western blot of representative *USP9X* immunoprecipitation experiment from control and *USP9X* variant fibroblast lysates. Immunoprecipitated proteins from $n = 3$ independent experiments (see Figure S10 in Supplement 1) were analyzed by tandem-mass-tag mass spectrometry for quantitation. **(E)** Relative protein quantities of significantly enriched *USP9X* interactors (enriched in *USP9X* immunoprecipitates (IPs) compared with immunoglobulin G (IgG) immunoprecipitates in control cells) in variant *USP9X* immunoprecipitation experiments. The p values were calculated via paired Student's t test. **(F)** Representative Western blot analysis of *USP9X* substrates implicated in neurodevelopmental signaling pathways in control and variant *USP9X* fibroblast cell lines. **(G)** Quantitation of Western blots in panel C and replicates experiments ($n = 3$ experiments) (Figure S8 in Supplement 1). Values represent relative abundance compared that in with control subjects ($n = 3$ cell lines); values underlined are significantly reduced (p values were obtained via Student's t test). * $p < .05$. β -Catenin, catenin beta-1; DAPI, 4',6-diamidino-2-phenylindole; DLAT, dihydroliipoamide S-acetyltransferase; FNBP1L, formin-binding protein 1-like; HMG2, high mobility group nucleosomal binding domain 2; ITCH, itchy E3 ubiquitin protein ligase; KCTD9, potassium channel tetramerization domain containing 9; MCL1, MCL1 apoptosis regulator, BCL2 family member; MINDBOMB, mindbomb E3 ubiquitin protein ligase 1; MW, molecular weight; RAPTOR, regulatory-associated protein of mammalian target of rapamycin; ROCK2, rho-associated protein kinase 2; RPS7, ribosomal protein S7; SMAD4, SMAD family member 4; SMURF1, SMAD specific E3 ubiquitin protein ligase 1; *USP9X*, ubiquitin specific peptidase 9 X-linked.

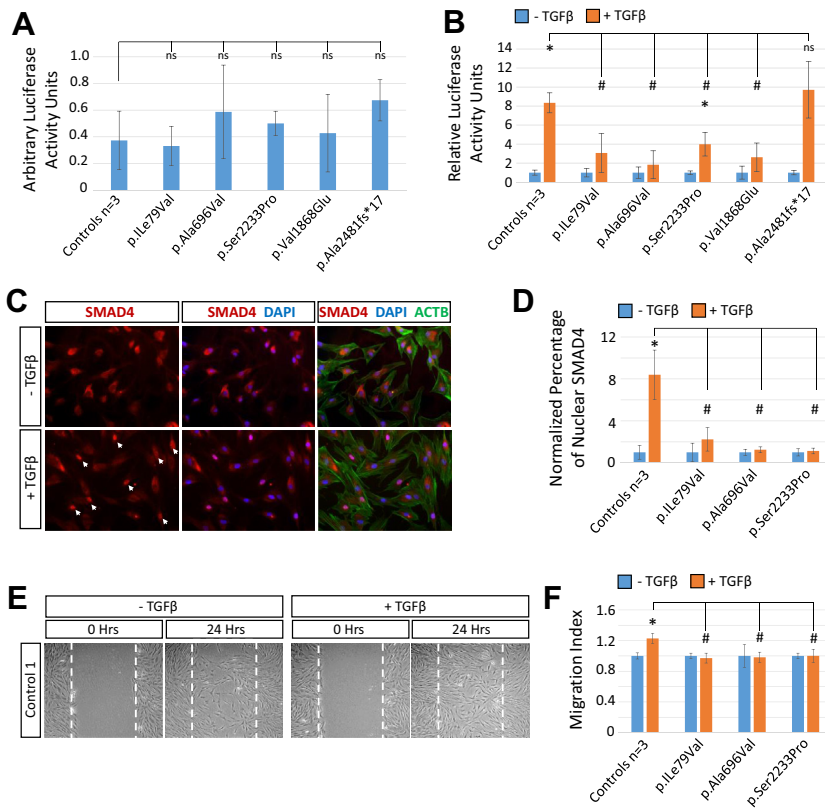


Figure 4. Transforming growth factor β (TGF β) signaling is disrupted in *USP9X* variant fibroblast cell lines. Cells were serum starved (0.2% serum) for 16 hours prior to the addition of TGF β and were assayed 24 hours later. **(A)** In the absence of added TGF β , cells display similar basal levels of signaling, as assessed by TGF β luciferase reporter assay. **(B)** Relative increase of TGF β signaling following addition of ligand as assessed by TGF β luciferase reporter assays. Experiment done in quadruplicate. **(C)** Representative immunofluorescent images of SMAD family member 4 (SMAD4) localization before (time = 0 hour) and after (time = 24 hours) the addition of TGF β . Arrowheads indicate nuclear localization. **(D)** Quantitation of SMAD4 nuclear translocation following the addition of TGF β . $n = 5$ replicates. **(E)** Representative images of scratch migration assay. **(F)** Quantitation of the relative stimulation of migration of cells into the scratch area following the addition of TGF β . $n = 3$ technical \times 3 biological replicates. *Statistical difference between \pm TGF β . #Statistical difference between controls and *USP9X* variant cell lines. ** $p < .05$, Student's t test. ACTB, actin B; DAPI, 4',6-diamidino-2-phenylindole; n.s., nonsignificant difference between controls and *USP9X* variant cell lines.

USP9X Missense Variants Lead to a Loss of TGF β Signaling

As SMURF1 levels were reduced across *USP9X* variant fibroblast lines, we assessed TGF β signaling capacity. Basal levels of signaling assessed by TGF β luciferase reporter assays were not affected (Figure 4A and Figure S13 in Supplement 1). The addition of TGF β resulted in an approximately 8-fold increase in luciferase activity in control cells and in the p.Ala2481fs*17 cell line in which the variant isoform is barely expressed (Figure 4B and Figures S5 and S13 in Supplement 1). In contrast, only a 2- to 4-fold induction was observed in the remaining inherited variant cell lines. A similar result was obtained from a cell line derived from participant USA1 harboring the de novo likely pathogenic variant p.Val1868Glu (Figure 4B and Figure S13 in Supplement 1). We tested TGF β signaling further using the inherited variant cell lines. SMAD4 is translocated into the nucleus during TGF β signaling, and an approximately 8-fold increase in nuclear SMAD4 was identified in control cells following TGF β stimulation, which is a significantly greater increase than that in the variant cell lines tested (Figure 4C, D and Figure S14 in Supplement 1). Lastly, we conducted a scratch migration assay to determine whether variant cell lines are induced to migrate in response to TGF β (19,34). The TGF β -stimulated migration in control cells (~20% increase) was not observed in variant cells (Figure 4E, F and Figure S15 in Supplement 1). In addition, we tested mTOR signaling capacity specifically in the p.Ala696Val cell lines ($n = 2$ brothers) in which RAPTOR levels were reduced (Figure 4C, D and Figure S8 in

Supplement 1). Across 2 independent assays involving either a standard or serum-stimulated cell culture protocol, the p.Ala696Val variant cell lines displayed evidence of a reduced mTOR response as assessed by reduced phospho-S6 ribosomal protein levels and reduced phospho-S6:S6 ribosomal protein ratio (Figure S16 in Supplement 1). We await additional cell lines with this variant or phenotype for more rigorous testing.

Collectively, these data provide functional support for pathogenicity of 3 inherited *USP9X* missense variants, p.Ile79Val, p.Ala696Val, and p.Ser2233Pro, and reveal that the strongest impact of these variants was on neurodevelopmental signaling pathways.

Loss of *Usp9x* Function Causes Learning and Memory Deficits in Mice

Our collective data on *USP9X* variants to date in male and female subjects suggest partial LOF as the initial molecular driver of the associated pathology. To support this hypothesis, we interrogated the phenotypic consequence of *Usp9x* deficiency in mice. We mated floxed *Usp9x* allelic mice with *Emx1-Cre* driver mice to delete *Usp9x* in the embryonic forebrain as previously described (17,18). Unlike in humans, *Usp9x* is subjected to X inactivation in mice (35), and as such we forwent studies in heterozygous female offspring and studied hemizygous deletion in male mice (compared with wild-type male littermates). These mice, herein referred to as "knockout mice," survive and provide opportunity to study

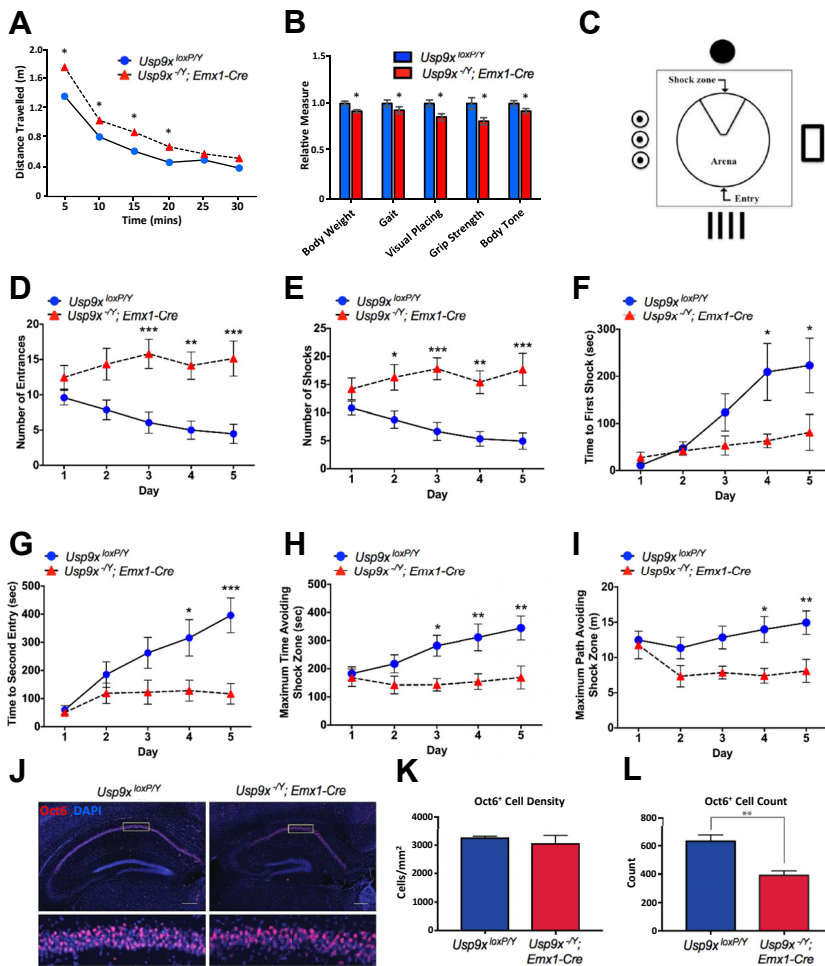


Figure 5. Behavioral deficits in *Usp9x* knockout mice. **(A)** Adult *Usp9x* forebrain-specific knockout mice (*Usp9x^{-/-}; Emx1-Cre*) travel farther than wild-type littermate controls (*Usp9x^{loxP/Y}*) in an open field test. **(B)** Knockout mice also exhibited significant differences in various parameters of the modified SHIRPA (SmithKline Beecham Pharmaceuticals; Harwell, MRC Mouse Genome Centre and Mammalian Genetics Unit; Imperial College School of Medicine at St. Mary's; Royal London Hospital, St. Bartholomew's and the Royal London School of Medicine phenotype assessment) neurological screening protocol (also see Table S4 in Supplement 2); the *p* values were calculated via 2-tailed unpaired *t* test. **(C)** Schematic of the Active Place Avoidance (APA) arena. **(D–I)** Knockout mice exhibited significantly reduced performance on different aspects of the APA task. Statistics relate to comparisons between wild-type and knockout animals on individual days of the 5 day test. Two-way analysis of variance (also see Figure S16 in Supplement 1). **(J–L)** Coronal sections of adult wild-type (left 2 panels) and mutant (right 2 panels) mice at the level of the hippocampus. Oct6 (red) was used as a marker for CA1 hippocampal neurons, and 4',6-diamidino-2-phenylindole (DAPI; blue) was used to label nuclei. Whereas the density of Oct6-expressing neurons was not different between control and mutant animals (panel K), the total number of Oct6-expressing neurons per CA1 region was reduced within the hippocampus of mutant animals. The *p* values were calculated via Student's *t* test. Scale bar in panel (J) low-magnification images = 250 μm. Scale bar in panel (J) high-magnification images = 30 μm. **p* < .05, ***p* < .01, ****p* < .001.

behavior. At postnatal day 60, we subjected knockout mice to a broad modified SHIRPA (SmithKline Beecham Pharmaceuticals; Harwell, MRC Mouse Genome Centre and Mammalian Genetics Unit; Imperial College School of Medicine at St. Mary's; Royal London Hospital, St. Bartholomew's and the Royal London School of Medicine phenotype assessment) phenotype screen (see Methods and Materials, Figure 5A, B, and Table S5 in Supplement 1) (22). Knockout mice displayed a significant increase in distance traveled in an open field test (Figure 5A) and exhibited deficits in weight, gait, grip strength, and visual placing (Figure 5B). Body position was also altered (less likely to be rearing or jumping), while no significant difference between control and knockout mice was identified for all other tests (Table S5 in Supplement 1).

Next, we interrogated hippocampal-dependent cognitive function using the Active Place Avoidance (APA) test (23). This test assesses the capacity to learn and remember the position of a fixed shock zone within a rotating platform, using visual cues (Figure 5C). No significant differences in behavior were observed during the APA habituation phase (Figure S17 in Supplement 1). Total distance traveled and average speed were also comparable over the test period (Figure S17B, C in Supplement 1). Knockout mice did, however, display

significantly reduced performance across a variety of test parameters in the APA task, including number of entrances into the shock zone (Figure 5D), total number of shocks (Figure 5E), latency to first shock (a measure of long-term memory) (Figure 5F), latency to second entry to the shock zone (a measure of short-term memory) (Figure 5G), maximum time, and path avoiding the shock zone (Figure 5H, I). Moreover, intragenotype analyses revealed that wild-type mice showed significant improvements in learning the avoidance task, while knockout mice did not (Figure S17D–I in Supplement 1). As the APA test is highly dependent on the CA1 region of the hippocampus, we assessed CA1 cellular architecture. Analysis revealed reduced total numbers of CA1 neurons in knockout mice, albeit at equivalent density (Figure 5J–L). Collectively, these data show that complete *Usp9x* LOF severely impacts hippocampal-dependent learning and memory, with additional (central nervous system-derived) motor, muscular, and visual defects in adult mice.

DISCUSSION

Our study redefines the molecular and clinical effects of rare *USP9X* variants that are predicted to be deleterious in male

individuals. Through integrated studies of patient-derived cell lines, and with evidence of learning and memory deficits of knockout mice, we conclude that DNA variation in *USP9X* leading to partial LOF has detrimental effects on normal brain development.

Prior to this study, only 4 male *USP9X* variants had been associated with pathogenicity in participants with limited clinical information (4,5). Here we report an additional 12 likely pathogenic cases. Although further clinically actionable information cannot be solely provided by *in silico* predictive tools, we discovered and used the best *USP9X*-centric tools to provide support of pathogenicity to approximately half of our cohort of VUSs. This proportion aligned with the prevalence of the clinical attributes as defined by our likely pathogenic cohort. Taken together, our work provides incentive and framework for clinical and genetic studies aimed at resolving these cases.

We characterize the *USP9X* clinical presentation in male subjects. Some features, including global developmental delay, ID, hypotonia, motor and speech delay, and brain abnormalities including thin corpus callosum and cerebellar defects, overlap with the more clearly defined female *USP9X* syndrome (3); however, consistent congenital features found in female subjects were rare or absent in male subjects. This difference is likely due to differing molecular consequences acting downstream of the mutation type: In female subjects, mutations cause loss of *USP9X* dosage (with potential to affect all substrates) compared with missense mutations in male subjects (including those inherited through apparently asymptomatic mothers), which involve disruption to particular subsets of substrates. The shared core neurological features between male and female subjects do, however, suggest a convergent mechanism of pathology, despite the differing mutation types. While it remains to be tested in female subjects, we speculate that disruption to TGF β is a prime candidate, whereby either reduced *USP9X* dosage (female subjects) or missense mutation (male subjects) may culminate in a loss of TGF β signaling in brain, stemming from a loss of key *USP9X* substrate(s) involved in signal transduction. Disrupted TGF β signaling has been implicated in several NDDs (36) and is involved in multiple aspects of brain development and function (37–40). *USP9X* joins an emerging group of X-linked genes, including *DDX3X*, *IQSEC2*, *KDM5C*, *SMC1A*, *ALG13*, and *OFD1*, that 1) escape X inactivation, 2) feature *de novo* heterozygous LOF mutations in female subjects with NDDs, and 3) feature missense variants with milder allelic impact (e.g., partial LOF) in male subjects with NDDs, which are often maternally inherited (41–46).

The hippocampus plays significant roles in learning and memory and in human ID and NDDs, and we discovered hippocampal-dependent learning and memory deficits in *Usp9x* knockout mice (47–50). Reductions in grip strength, body tone, gait, and visual placement also phenocopies hypotonia, motor deficits, and visual defects seen in humans. Previous studies in mice revealed several brain malformations, including agenesis of the corpus callosum, dilated ventricles (ventriculomegaly), and other brain malformations, which we now show are frequent in human male subjects (18). The remarkable phenotypic similarities between human and mouse

models have two implications. First, they align the mechanism of *USP9X* missense variation in male subjects with partial LOF. We appreciate that the mouse is a complete LOF model with a comparatively severe phenotype, and analogous germline complete LOF mutations in humans (i.e., hemizygous or homozygous) are not likely compatible with life (2). Nevertheless, the similarities between human subjects and the knockout mice suggest the variants hinder specific *USP9X* brain functions. Second, because a brain LOF mechanism is suggested, we speculate that the cellular and molecular mechanisms resolved in knockout mice may indeed be relevant to human pathology.

Using this same *Usp9x* knockout mice model, we previously established that loss of *Usp9x* results in decreased TGF β -mediated axonogenesis (18), decreased mTOR-mediated neural stem cell proliferation (7), and differentiation defects associated with defective Wnt and Notch signaling (12). As *USP9X* variant cell lines were refractory to TGF β stimulation, it is plausible that loss of axonal tracts (e.g., agenesis of the corpus callosum) stems in part from defective TGF β signaling. *USP9X* has several substrates involved in regulating the TGF β pathway, including *SMURF1*, *SMAD4*, and Praja ring finger ubiquitin ligase 1 (6,9,15). In our male participants, we observed evidence of both downregulation of *SMURF1* and loss of nuclear localization of *SMAD4*. Both phenomena are consistent with a loss of *USP9X* interaction and may drive defective TGF β signaling, but they may alternatively reflect loss of TGF β signaling stemming from other molecular calamities downstream of *USP9X*. Indeed, it is intriguing that the variants tested in these assays are located in divergent regions of the protein that are predicted to mediate distinct protein–protein interactions. Thus, while all tested variants caused a loss of TGF β signaling, the key substrates driving this effect may differ. We provide evidence that different variants can uniquely impact various *USP9X* substrate interactions. For example, only the p.Ala696Val variant cell lines had reduced RAPTOR and myeloid cell leukemia sequence 1 protein levels, with loss of RAPTOR correlating with evidence of reduced mTOR activity. Thus, the p.Ala696Val variant resulted in both defective TGF β and mTOR signaling, and it was associated with the two most severely affected participants. *USP9X* has also other substrates that are encoded by genes whose LOF are associated with NDDs (*CTNBN1*, *ITCH*, *NUAK1*, *PEX5*, *SMAD4*, *SMURF1*, *DCX*, *MIB1*, *SOX2*, *HERC2*, *NONO*, *RPGRIP1L*, *PRICKLE1*, *PRICKLE2*, *MTORC1*) (1). Importantly, *USP9X* functions upstream of all these substrates by maintaining their stability (and hence function) via deubiquitylation, and therefore, any loss of interaction between *USP9X* and the substrate has potential to cause the neurodevelopmental pathology associated with that substrate.

USP9X sits at the hub of a protein interactome network enriched with NDD genes. It is also known that *USP9X* regulates processes relevant to NDDs, including neurogenesis, migration, neurite growth, and synaptogenesis, through this NDD network. Resolving the molecular, cellular, and developmental pathologies underpinning *USP9X* variants is likely to converge on pathologies of NDDs of diverse genetic origins and potentially offer a point for intervention.

ACKNOWLEDGMENTS AND DISCLOSURES

This work was supported by Simons Foundation Autism Research Initiative (SFARI Explorer Grant No. 527556 to [MPI, SW, LJ]), Australian Research Council (Grant No. ARC DE160100620 [to LJ]), the National Health and Medical Research Council of Australia (Program Grant No. 628952 and Research Fellowship 1041920 [to JG]), National Institute of Health (Grant NO. R01MH107182 [to PP]). USA 26 was evaluated through the Duke Genome Sequencing Clinic, supported by the Duke University Health System and partially funded by UCB Celltech.

CL-O and OS-F were supported by Programa EDP SOLIDARIA 2016 (Fundación EDP). DCK, DB, and TMM were supported by The Research Institute, Nationwide Children's Hospital. TMP was funded by the Cedars-Sinai Diana and Steve Marienhoff Fashion Industries Guild Endowed Fellowship in Pediatric Neuromuscular Diseases and the Undiagnosed Diseases Program. The DDD study presents independent research commissioned by the Health Innovation Challenge Fund (Grant No. HICF-1009-003), a parallel funding partnership between Wellcome and the Department of Health, and the Wellcome Sanger Institute (Grant No. WT098051). The views expressed in this publication are those of the author(s) and not necessarily those of Wellcome or the Department of Health. The study has UK Research Ethics Committee approval (10/H0305/83, granted by the Cambridge South REC, and GEN/284/12 granted by the Republic of Ireland REC). The research team acknowledges the support of the National Institute for Health Research, through the Comprehensive Clinical Research Network. This study makes use of DECIPHER (<http://decipher.sanger.ac.uk>), which is funded by the Wellcome Trust.

We are grateful for the support and contributions of all families involved in this study. We are thankful for the funding received from Creola Pora with the help of her friends and colleagues.

IC, MPa, and MA are employees of UCB. JAR belongs to the Department of Molecular and Human Genetics at Baylor College of Medicine, which receives revenue from clinical genetic testing conducted at Baylor Genetics Laboratories. LAP-J is scientific advisor and founding partner of qGenomics Laboratory. CL-O is a scientific advisor and shareholder of DreamGenics Ltd. All other authors report no biomedical financial interests or potential conflicts of interest.

ARTICLE INFORMATION

From the University of Adelaide and Robinson Research Institute, Adelaide (BVJ, RK, AI, AGa, DD, MC, LAP-J, JG, LAJ); Women's and Children's Hospital (LAP-J), Adelaide; and South Australian Health and Medical Research Institute (LAP-J, JG), Adelaide, South Australia; School of Biomedical Sciences (SO, MK, MPI) and Queensland Brain Institute (SAI, MSV, TB, MPI), The University of Queensland; Griffith Institute for Drug Discovery (MK, SAW), Griffith University, Brisbane; Queensland Centre for Mental Health Research (SAI, TB), Wacol, Queensland, Australia; Bio-Frontiers Institute (AI), University of Colorado Boulder, Boulder, Colorado; Department of Physiology (EP, SY, PP), Northwestern University Feinberg School of Medicine, Chicago, Illinois; Children's Hospital of Philadelphia (AGo, EZ, CM, EB, PK, DL); Translational Medicine & Human Genetics (SAs), Hospital of the University of Pennsylvania, Philadelphia; Children's Hospital of Pittsburgh (SM-K, EI), Pittsburgh, Pennsylvania; Center for Rare Childhood Disorders (VN, KR), Translational Genomics Research Institute, Phoenix, Arizona; Division of Human Genetics (LPe), Cincinnati Children's Hospital; Department of Pediatrics, University of Cincinnati College of Medicine, Cincinnati; Nationwide Children's Hospital (DCK, DB, TMM); Department of Pediatrics (SHE), The Ohio State University College of Medicine, Columbus, Ohio; Department of Pediatrics (VS, KSc, JAS), Division of Medical Genetics, Duke University Medical Center, Durham; Division of Pediatric Genetics and Metabolism (YP-Y, LDS), University of North Carolina, Chapel Hill, North Carolina; Department of Clinical Genomics (FPeV, PNP, SAE, EWK), Center for Individualized Medicine (FPeV), and Department of Laboratory Medicine and Pathology (SSB), Mayo Clinic, Rochester, Minnesota; Jane and John Justin Neuroscience Center (MSP), Cook Children's Medical Center, Fort Worth; Department of Pediatrics (MKK), University of Texas Medical School at Houston; Baylor College of Medicine (JAR), Houston, Texas; Division of Genetics (CEK, JLS),

Department of Pediatrics, University of Michigan, Ann Arbor, Michigan; Medical Genetics Unit (AEL, MAS), Mass General Hospital for Children, Boston, Massachusetts; David Geffen School of Medicine (CS), University of California–Los Angeles; Department of Pediatrics (PAS-L, JMGJr, MAU, TMP) and Department of Neurology and the Board of Governors Regenerative Medicine Institute (TMP), Cedars-Sinai Medical Center, Los Angeles; Department of Genetics (KT), Kaiser Permanente, Sacramento, California; Section of Genetics and Metabolism (GBS) and Department of Genetic Counseling (NRD), University of Arkansas for Medical Sciences, Little Rock, Arkansas; Department of Pediatrics (AAs, KEJ), University of Louisville School of Medicine, Louisville, Kentucky; Clinical Genetics Services (NY), Department of Pediatrics, New York University School of Medicine, New York, New York; Department of Medical Genetics (TO), British Columbia Women's Hospital and University of British Columbia; Department of Medical Genetics (MVA), University of British Columbia, Vancouver, British Columbia; Children's Hospital of Eastern Ontario (ML), Ottawa; Division of Clinical and Metabolic Genetics (SM-A), Department of Pediatrics, University of Toronto, The Hospital for Sick Children, Toronto, Ontario, Canada; Oxford Centre for Genomic Medicine (HL, UK), Oxford University Hospitals National Health Services Foundation Trust, Oxford; Translational Medicine (IC), UCB Pharma, Slough, United Kingdom; Center for Rare Diseases (SG), Department of Pediatrics and Department of Clinical Genetics, University Hospital Copenhagen, Copenhagen, Denmark; Service de Génétique Médicale (SM, SK, SB), Centre Hospitalier Universitaire Nantes and l'Institut du Thorax, Institut National de la Santé et de la Recherche Médicale, Centre National de la Recherche Scientifique, Université de Nantes, Nantes; Service de Génétique Clinique (LPa), Centre de Référence Déficiences Intellectuelles de Causes Rares, Centre Hospitalier Universitaire Hôpital Sud, Rennes; Centre Hospitalier Régional Universitaire de Tours (MR), Service de Génétique, Unité Nixte de Recherche 1253, iBrain, Université de Tours, Institut National de la Santé et de la Recherche Médicale, Tours; Groupe de Recherche Clinique No. 19 (AAf), ConCer-LD, Département de Génétique, Assistance Publique–Hôpitaux de Paris, Hôpital Armand Trousseau, Centres de Référence Maladies Rares des Déficiences Intellectuelles de Causes Rares, and Sorbonne Université (TBdV), Groupe de Recherche Clinique No. 19, ConCer-LD, Neuropédiatrie, Centres de Référence Maladies Rares Neurogénétique, Institut National de la Santé et de la Recherche Médicale, Assistance Publique–Hôpitaux de Paris, Hôpital Armand Trousseau; and Hôpital de la Pitié-Salpêtrière (BK), Département de Génétique, Paris; Centre de Génétique Humaine (LVM), Université de Franche-Comté, Besançon, France; Erasme University Hospital (JD, MM), Université Libre de Bruxelles, Brussels, Translational Medicine (MPa, MA), UCB Pharma, Braine-l'Alleud, Belgium; Institute of Human Genetics (ND), Heidelberg University, Heidelberg, Germany; Department of Human Genetics (DAK, TK), Radboud University Medical Center, Nijmegen; Department of Metabolic Diseases (PMVH) and Department of Genetics (RO, EvB, BvdZ), University Medical Center Utrecht, Utrecht; Department of Clinical Genetics (MW), Vrije Universiteit University Medical Center, Amsterdam; Department of Clinical Genetics (NdH, MJVH), Leiden University Medical Center, Leiden; Department of Clinical Genetics (MRFr), Maastricht University Medical Center, Maastricht; Department of Clinical Genetics (SD), Erasmus University Medical Center, Rotterdam, The Netherlands; Medical Genetics Unit (PZ, JS, CFR), Hospital Pediátrico, Centro Hospitalar e Universitário de Coimbra, Coimbra, Portugal; Departamento de Bioquímica y Biología Molecular (CL-O, OS-F), Instituto Universitario de Oncología del Principado de Asturias, Universidad de Oviedo, Oviedo; Centro de Investigación Biomédica en Red de Cáncer (CL-O); Unidad de Neurología Infantil (AF-J), Hospital Universitario Quirón Madrid, Madrid; Hospital del Mar Research Institute (LAP-J), Network Research Centre for Rare Diseases and Universitat Pompeu Fabra, Barcelona, Spain; Institute of Medical Genetics (AR, KSt, PJ), University of Zurich, Schlieren, Switzerland; and Department of Medical Genetics (MFS), University Hospital of North Norway, Tromsø, Norway.

Authors from the Undiagnosed Diseases Network include Loren Pena, Vandana Shashi, Kelly Schoch and Jennifer A. Sullivan. We acknowledge the contributions of other collaborating members: Maria T. Acosta, David R. Adams, Aaron Aday, Mercedes E. Alejandro, Patrick Allard, Euan A. Ashley, Mahshid S. Azamian, Carlos A. Bacino, Guney Bademci, Eva Baker, Ashok Balasubramanyam, Dustin Baldrige, Deborah Barbouth, Gabriel F. Batzli, Alan H. Beggs, Hugo J. Bellen, Jonathan A. Bernstein, Gerard T. Berry, Anna

Bican, David P. Bick, Camille L. Birch, Stephanie Bivona, Carsten Bonnenmann, Devon Bonner, Braden E. Boone, Bret L. Bostwick, Lauren C. Briere, Ely Brokamp, Donna M. Brown, Matthew Brush, Elizabeth A. Burke, Lindsay C. Burrage, Manish J. Butte, Olveen Carrasquillo, Ta Chen Peter Chang, Hsiao-Tuan Chao, Gary D. Clark, Terra R. Coakley, Laurel A. Cobban, Joy D. Cogan, F. Sessions Cole, Heather A. Colley, Cynthia M. Cooper, Heidi Cope, William J. Craigen, Precilla D'Souza, Surendra Dasari, Mariska Davids, Jean M. Davidson, Jyoti G. Dayal, Esteban C. Dell'Angelica, Shweta U. Dhar, Naghme Dorrani, Daniel C. Dorset, Emilie D. Douine, David D. Draper, Annika M. Dries, Laura Duncan, David J. Eckstein, Lisa T. Emrick, Christine M. Eng, Gregory M. Enns, Cecilia Esteves, Tyra Estwick, Liliana Fernandez, Carlos Ferreira, Elizabeth L. Fieg, Paul G. Fisher, Brent L. Fogel, Irman Forghani, Noah D. Friedman, William A. Gahl, Rena A. Godfrey, Alicia M. Goldman, David B. Goldstein, Jean-Philippe F. Gourdine, Alana Grajewski, Catherine A. Groden, Andrea L. Gropman, Melissa Haendel, Rizwan Hamid, Neil A. Hanchard, Frances High, Ingrid A. Holm, Jason Hom, Alden Huang, Yong Huang, Rosario Isasi, Fariha Jamal, Yong-hui Jiang, Jean M. Johnston, Angela L. Jones, Lefkothea Karaviti, Emily G. Kelley, David M. Koeller, Isaac S. Kohane, Jennefer N. Kohler, Deborah Krakow, Donna M. Krasnewich, Susan Korrick, Mary Koziura, Joel B. Krier, Jennifer E. Kyle, Seema R. Lalani, Byron Lam, Brendan C. Lanpher, Ian R. Lanza, C. Christopher Lau, Jozef Lazar, Kimberly LeBlanc, Brendan H. Lee, Hane Lee, Roy Levitt, Shawn E. Levy, Richard A. Lewis, Sharyn A. Lincoln, Pengfei Liu, Xue Zhong Liu, Sandra K. Loo, Joseph Loscalzo, Richard L. Maas, Ellen F. Macnamara, Calum A. MacRae, Valerie V. Maduro, Marta M. Majcherska, May Christine V. Malicdan, Laura A. Mamounas, Teri A. Manolio, Thomas C. Markello, Ronit Marom, Martin G. Martin, Julian A. Martinez-Agosto, Shruti Marwaha, Thomas May, Jacob McCauley, Allyn McConkie-Rosell, Colleen E. McCormack, Alexa T. McCray, Jason D. Merker, Thomas O. Metz, Matthew Might, Eva Morava-Kozicz, Paolo M. Moretti, Marie Morimoto, John J. Mulvihill, David R. Murdock, Avi Nath, Stan F. Nelson, J. Scott Newberry, John H. Newman, Sarah K. Nicholas, Donna Novacic, Devin Oglesbee, James P. Orengo, Stephen Pak, J. Carl Pallais, Christina GS. Palmer, Jeanette C. Papp, Neil H. Parker, John A. Phillips III, Jennifer E. Posey, John H. Postlethwait, Lorraine Potocki, Barbara N. Pusey, Genecee Renteri, Chloe M. Reuter, Lynette Rives, Amy K. Robertson, Lance H. Rodan, Jill A. Rosenfeld, Robb K. Rowley, Ralph Sacco, Jacinda B. Sampson, Susan L. Samson, Mario Saporta, Judy Schaechter, Timothy Schedl, Daryl A. Scott, Lisa Shakachite, Prashant Sharma, Kathleen Shields, Jimann Shin, Rebecca Signer, Catherine H. Sillari, Edwin K. Silverman, Janet S. Sinshheimer, Kevin S. Smith, Lilianna Solnica-Krezel, Rebecca C. Spillmann, Joan M. Stoler, Nicholas Stong, David A. Sweetser, Cecelia P. Tamburro, Queenie K.-G. Tan, Mustafa Tekin, Fred Telischi, Willa Thorson, Cynthia J. Tift, Camilo Toro, Alyssa A. Tran, Tiina K. Urv, Tiphonie P. Vogel, Daryl M. Waggott, Colleen E. Wahl, Nicole M. Walley, Chris A. Walsh, Melissa Walker, Jennifer Wambach, Jijun Wan, Lee-kai Wang, Michael F. Wangler, Patricia A. Ward, Katrina M. Waters, Bobbie-Jo M. Webb-Robertson, Daniel Wegner, Monte Westerfield, Matthew T. Wheeler, Anastasia L. Wise, Lynne A. Wolfe, Jeremy D. Woods, Elizabeth A. Worthey, Shinya Yamamoto, John Yang, Amanda J. Yoon, Guoyun Yu, Diane B. Zastrow, Chunli Zhao and Stephan Zuchner. The principal investigator of the Undiagnosed Disease Network is William Gahl (gahlw@mail.nih.gov).

BVJ and RK contributed equally to this work.

Address correspondence to Lachlan A. Jolly, Ph.D., 4 North Terrace, Level 8 Adelaide Health and Medical School Building, The University of Adelaide, Adelaide, SA 5005, Australia; E-mail: Lachlan.Jolly@adelaide.edu.au; and Jozef Gécz, Ph.D., 4 North Terrace, Level 8 Adelaide Health and Medical School Building, The University of Adelaide, Adelaide, SA 5005, Australia; E-mail: Jozef.Gecz@adelaide.edu.au.

Received Mar 27, 2019; revised May 23, 2019; accepted May 30, 2019.

Supplementary material cited in this article is available online at <https://doi.org/10.1016/j.biopsych.2019.05.028>.

REFERENCES

- Murtaza M, Jolly LA, Gécz J, Wood SA (2015): La FAM fatale: USP9X in development and disease. *Cell Mol Life Sci* 72:2075–2089.
- Pantaleon M, Kanai-Azuma M, Mattick JS, Kaibuchi K, Kaye PL, Wood SA (2001): FAM deubiquitylating enzyme is essential for pre-implantation mouse embryo development. *Mech Dev* 109:151–160.
- Reijnders MR, Zachariadis V, Latour B, Jolly L, Mancini GM, Pfundt R, *et al.* (2016): De novo loss-of-function mutations in USP9X cause a female-specific recognizable syndrome with developmental delay and congenital malformations. *Am J Hum Genet* 98:373–381.
- Homan CC, Kumar R, Nguyen LS, Haan E, Raymond FL, Abidi F, *et al.* (2014): Mutations in USP9X are associated with X-linked intellectual disability and disrupt neuronal cell migration and growth. *Am J Hum Genet* 94:470–478.
- Paemka L, Mahajan VB, Ehaideb SN, Skeie JM, Tan MC, Wu S, *et al.* (2015): Seizures are regulated by ubiquitin-specific peptidase 9 X-linked (USP9X), a de-ubiquitinase. *PLoS Genet* 11:e1005022.
- Agrawal P, Chen YT, Schilling B, Gibson BW, Hughes RE (2012): Ubiquitin-specific peptidase 9, X-linked (USP9X) modulates activity of mammalian target of rapamycin (mTOR). *J Biol Chem* 287:21164–21175.
- Bridges CR, Tan MC, Premarathne S, Nanayakkara D, Bellette B, Zencak D, *et al.* (2017): USP9X deubiquitylating enzyme maintains RAPTOR protein levels, mTORC1 signalling and proliferation in neural progenitors. *Sci Rep* 7:391.
- Chen X, Zhang B, Fischer JA (2002): A specific protein substrate for a deubiquitinating enzyme: Liquid facets is the substrate of Fat facets. *Genes Dev* 16:289–294.
- Dupont S, Mamidi A, Cordenonsi M, Montagner M, Zacchigna L, Adorno M, *et al.* (2009): FAM/USP9x, a deubiquitinating enzyme essential for TGFbeta signaling, controls Smad4 monoubiquitination. *Cell* 136:123–135.
- Mouchantaf R, Azakir BA, McPherson PS, Millard SM, Wood SA, Angers A (2006): The ubiquitin ligase itch is auto-ubiquitylated in vivo and in vitro but is protected from degradation by interacting with the deubiquitylating enzyme FAM/USP9X. *J Biol Chem* 281:38738–38747.
- Overstreet E, Fitch E, Fischer JA (2004): Fat facets and Liquid facets promote Delta endocytosis and Delta signaling in the signaling cells. *Development* 131:5355–5366.
- Premarathne S, Murtaza M, Matigian N, Jolly LA, Wood SA (2017): Loss of Usp9x disrupts cell adhesion, and components of the Wnt and Notch signaling pathways in neural progenitors. *Sci Rep* 7:8109.
- Taya S, Yamamoto T, Kanai-Azuma M, Wood SA, Kaibuchi K (1999): The deubiquitinating enzyme Fam interacts with and stabilizes beta-catenin. *Genes Cells* 4:757–767.
- Tseng LC, Zhang C, Cheng CM, Xu H, Hsu CH, Jiang YJ (2014): New classes of mind bomb-interacting proteins identified from yeast two-hybrid screens. *PLoS One* 9:e93394.
- Xie Y, Avello M, Schirle M, McWhinnie E, Feng Y, Bric-Furlong E, *et al.* (2013): Deubiquitinase FAM/USP9X interacts with the E3 ubiquitin ligase SMURF1 protein and protects it from ligase activity-dependent self-degradation. *J Biol Chem* 288:2976–2985.
- Jolly LA, Taylor V, Wood SA (2009): USP9X enhances the polarity and self-renewal of embryonic stem cell-derived neural progenitors. *Mol Biol Cell* 20:2015–2029.
- Oishi S, Premarathne S, Harvey TJ, Iyer S, Dixon C, Alexander S, *et al.* (2016): Usp9x-deficiency disrupts the morphological development of the postnatal hippocampal dentate gyrus. *Sci Rep* 6:25783.
- Stegeman S, Jolly LA, Premarathne S, Gecz J, Richards LJ, Mackay-Sim A, *et al.* (2013): Loss of Usp9x disrupts cortical architecture, hippocampal development and TGFbeta-mediated axonogenesis. *PLoS One* 8:e68287.
- Liang CC, Park AY, Guan JL (2007): In vitro scratch assay: A convenient and inexpensive method for analysis of cell migration in vitro. *Nat Protoc* 2:329–333.
- Jolly LA, Nguyen LS, Domingo D, Sun Y, Barry S, Hancarova M, *et al.* (2015): HCFC1 loss-of-function mutations disrupt neuronal and neural progenitor cells of the developing brain. *Hum Mol Genet* 24:3335–3347.
- Harris L, Dixon C, Cato K, Heng YH, Kumiawan ND, Ullmann JF, *et al.* (2013): Heterozygosity for nuclear factor one x affects hippocampal-dependent behaviour in mice. *PLoS One* 8:e65478.
- Rogers DC, Fisher EM, Brown SD, Peters J, Hunter AJ, Martin JE (1997): Behavioral and functional analysis of mouse phenotype: SHIRPA, a proposed protocol for comprehensive phenotype assessment. *Mamm Genome* 8:711–713.

23. Stuchlik A, Petrasek T, Prokopova I, Holubova K, Hatalova H, Vales K, *et al.* (2013): Place avoidance tasks as tools in the behavioral neuroscience of learning and memory. *Physiol Res* 62(suppl 1):S1–S19.
24. Firth HV, Richards SM, Bevan AP, Clayton S, Corpas M, Rajan D, *et al.* (2009): DECIPHER: Database of Chromosomal Imbalance and Phenotype in Humans Using Ensembl Resources. *Am J Hum Genet* 84:524–533.
25. Richards S, Aziz N, Bale S, Bick D, Das S, Gastier-Foster J, *et al.* (2015): Standards and guidelines for the interpretation of sequence variants: A joint consensus recommendation of the American College of Medical Genetics and Genomics and the Association for Molecular Pathology. *Genet Med* 17:405–424.
26. Zhang Q, Dong A, Walker JR, Bountra C, Arrowsmith CH, Edwards AM, *et al.* (2018): Crystal structure of a peptidase (2018). Available at: <http://www.rcsb.org/structure/5WCH>. Accessed June 2, 2018.
27. Wang K, Li M, Hakonarson H (2010): ANNOVAR: Functional annotation of genetic variants from high-throughput sequencing data. *Nucleic Acids Res* 38:e164.
28. Rentzsch P, Witten D, Cooper GM, Shendure J, Kircher M (2019): CADD: Predicting the deleteriousness of variants throughout the human genome. *Nucleic Acids Res* 47:D886–D894.
29. Pejaver V, Urresti J, Lugo-Martinez J, Pagel KA, Lin GN, Nam H, *et al.* (2017): MutPred2: Inferring the molecular and phenotypic impact of amino acid variants [published online ahead of print May 9]. *bioRxiv*.
30. Ebisawa T, Fukuchi M, Murakami G, Chiba T, Tanaka K, Imamura T, *et al.* (2001): Smurf1 interacts with transforming growth factor-beta type I receptor through Smad7 and induces receptor degradation. *J Biol Chem* 276:12477–12480.
31. Wiese KE, Nusse R, van Amerongen R (2018): Wnt signalling: Conquering complexity. *Development* 145(12).
32. Crino PB (2016): The mTOR signalling cascade: Paving new roads to cure neurological disease. *Nat Rev Neurol* 12:379–392.
33. Vucic D, Dixit VM, Wertz IE (2011): Ubiquitylation in apoptosis: A post-translational modification at the edge of life and death. *Nat Rev Mol Cell Biol* 12:439–452.
34. Schiller M, Javelaud D, Mauviel A (2004): TGF-beta-induced SMAD signaling and gene regulation: Consequences for extracellular matrix remodeling and wound healing. *J Dermatol Sci* 35:83–92.
35. Berletch JB, Ma W, Yang F, Shendure J, Noble WS, Distèche CM, *et al.* (2015): Escape from X inactivation varies in mouse tissues. *PLoS Genet* 11:e1005079.
36. Kashima R, Hata A (2018): The role of TGF- β superfamily signaling in neurological disorders. *Acta Biochim Biophys Sin (Shanghai)* 50:106–120.
37. Bialas AR, Stevens B (2013): TGF-beta signaling regulates neuronal C1q expression and developmental synaptic refinement. *Nat Neurosci* 16:1773–1782.
38. Gomes FC, Sousa Vde O, Romao L (2005): Emerging roles for TGF-beta1 in nervous system development. *Int J Dev Neurosci* 23:413–424.
39. Caraci F, Gulisano W, Guida CA, Impellizzeri AA, Drago F, Puzzo D, *et al.* (2015): A key role for TGF-beta1 in hippocampal synaptic plasticity and memory. *Sci Rep* 5:11252.
40. Fukushima T, Liu RY, Byrne JH (2007): Transforming growth factor-beta2 modulates synaptic efficacy and plasticity and induces phosphorylation of CREB in hippocampal neurons. *Hippocampus* 17:5–9.
41. Snijders Blok L, Madsen E, Juusola J, Gilissen C, Baralle D, Reijnders MR, *et al.* (2015): Mutations in DDX3X are a common cause of unexplained intellectual disability with gender-specific effects on Wnt signaling. *Am J Hum Genet* 97:343–352.
42. Shoubridge C, Harvey RJ, Dudding-Byth T (2019): IQSEC2 mutation update and review of the female-specific phenotype spectrum including intellectual disability and epilepsy. *Hum Mutat* 40:5–24.
43. Fieremans N, Van Esch H, de Ravel T, Van Driessche J, Belet S, Bauters M, *et al.* (2015): Microdeletion of the escape genes KDM5C and IQSEC2 in a girl with severe intellectual disability and autistic features. *Eur J Med Genet* 58:324–327.
44. Jansen S, Kleefstra T, Willemsen MH, de Vries P, Pfundt R, Hehir-Kwa JY, *et al.* (2016): De novo loss-of-function mutations in X-linked SMC1A cause severe ID and therapy-resistant epilepsy in females: Expanding the phenotypic spectrum. *Clin Genet* 90:413–419.
45. Epi KC, Epilepsy Phenome/Genome P, Allen AS, Berkovic SF, Cosssette P, Delanty N, *et al.* (2013): De novo mutations in epileptic encephalopathies. *Nature* 501:217–221.
46. Sakakibara N, Morisada N, Nozu K, Nagatani K, Ohta T, Shimizu J, *et al.* (2019): Clinical spectrum of male patients with OFD1 mutations. *J Hum Genet* 64:3–9.
47. Bostrom C, Yau SY, Majaess N, Vetrici M, Gil-Mohapel J, Christie BR (2016): Hippocampal dysfunction and cognitive impairment in Fragile-X Syndrome. *Neurosci Biobehav Rev* 68:563–574.
48. Penzes P, Buonanno A, Passafaro M, Sala C, Sweet RA (2013): Developmental vulnerability of synapses and circuits associated with neuropsychiatric disorders. *J Neurochem* 126:165–182.
49. Nadel L (2003): Down's syndrome: A genetic disorder in biobehavioral perspective. *Genes Brain Behav* 2:156–166.
50. Deboer T, Wu Z, Lee A, Simon TJ (2007): Hippocampal volume reduction in children with chromosome 22q11.2 deletion syndrome is associated with cognitive impairment. *Behav Brain Funct* 3:54.